Optimal counter-current exchange networks

Robert S. Farr*
The London Institute for Mathematical Sciences, 35a South Street, Mayfair, London W1K 2XF, United Kingdom and Unilever R&D, Colworth Science Park, Bedford MK44 1LQ, United Kingdom

Yong Mao†
School of Physics and Astronomy, University of Nottingham, Nottingham NG7 2RD, United Kingdom
(Received 16 February 2016; published 18 November 2016)

We present a general analysis of exchange devices linking their efficiency to the geometry of the exchange surface and supply network. For certain parameter ranges, we show that the optimal exchanger consists of densely packed pipes which can span a thin sheet of large area (an "active layer"), which may be crumpled into a fractal surface and supplied with a fractal network of pipes. We derive the efficiencies of such exchangers, showing the potential for significant gains compared to regular exchangers (where the active layer is flat), using parameters relevant to biological systems.

DOI: 10.1103/PhysRevE.94.052410

I. INTRODUCTION

The design of efficient exchange devices is an important problem in engineering and biology. A wide variety of heat exchangers, such as plate, coil, and counter-current, are employed in industrial settings [1], while in nature, leaf venation, blood circulation networks, gills, and lungs have evolved to meet multiple physiological imperatives. A distinctive feature of the biological examples is their complex, hierarchical (fractal) nature [2], with branching and usually anastomosing geometries [3,4]. It is clear that one reason for this is the possibility to include a large surface for exchange within a compact volume, as in the human lungs, which comprise an alveolar area greater than 50 m^2 [5]. However, maximal surface area is unlikely to be the only criterion for optimization [6,7]. As an example, West *et al.* have analyzed biological circulatory systems on the basis that power is minimized with the constraint that a minimum flux of respiratory fluid is brought to every cell in the volume of an organism, and were able to explain well known allometric scaling laws in biology [2].

Although scaling behaviors are known in some cases, the detailed geometry of optimal exchangers remains elusive. With the advance of new fabrication technologies such as three-dimensional printing [8], it is becoming possible to build structures of comparable complexity to biological systems, so there is a need not only to understand the principles and compromises upon which natural systems are based, but also for that understanding to be constructive, mapping system parameters to actual designs.

The analytic literature in this area has focused on heat transfer from a fluid to a solid body, with a particular emphasis on cooling of integrated circuits [9]. Branching fractal networks are much studied due to their ability to give good heat transfer with a low pressure drop [10,11] (although sometimes simpler geometries can be more efficient [12]), and multiscale structures are also found to have a high heat transfer density [13].

In this contribution, we consider exchange as a general process, which includes gas, solute, and heat exchange, and we look for the optimal designs which can ensure complete exchange (to be defined below) while requiring a minimum amount of mechanical power to generate the necessary fluid flows.

We use the language of thermal processes, since the relevant material properties have widely used notation. However, with a suitable translation of quantities, the analysis also applies to mass transfer. For example, in a thermal system with linear materials, the quantities temperature, heat, heat capacity per unit volume, and thermal conductivity would correspond in a system of gas exchange to partial pressure of gas, mass of gas, Henry's law coefficient and the product of the Henry's law coefficient, and gas diffusivity. For mass exchange with solutes, the analog of temperature would be osmotic pressure of the solute.

II. NONDIMENSIONALIZATION

The first step is to gather problem parameters into dimensionless groups, which span the space of possible exchange problems.

Suppose there are two counter-flowing (perhaps dissimilar) fluids with given properties: thermal conductivities κ_j ($j \in \{1,2\}$), heat capacities per unit volume C_j, and viscosities η_j. Let there be an imposed difference ΔT in the *inlet* temperatures, and an imposed volumetric flow rate Q_1 of fluid 1 (while we are free to choose Q_2). For example, if we are considering thermoelectric generation from the exhaust gases of a vehicle, Q_1 would be the volumetric flow of exhaust gases. Analogously, in gas exchange for vertebrate respiration, we take the required blood flow to the lungs or gills as the fixed quantity Q_1.

The fluid streams between which exchange occurs are assumed separated by walls of thickness w (taken to be the minimum consistent with biological or engineering constraints) and thermal conductivity κ_{wall}; the latter again an imposed constraint. We assume that the exchanger needs to

*robert.farr@unilever.com
†yong.mao@nottingham.ac.uk

be compact, in that it fits inside a roughly cubical volume of side length $L_{\max}$, and the pipes, being straight, are each of length $L \leqslant L_{\max}$. Last, we wish the exchange process to go to completion, in that the total exchanged power is of order $E_{\text{end}} = C_1 Q_1 \Delta T$, which results in the outlet temperature of flow 1 being equal to the inlet temperature of flow 2 (and conversely if the exchanger is "balanced," i.e., $Q_1 C_1 = Q_2 C_2$). Our aim is to find an exchange network which satisfies all these constraints (which we believe are a typical set for both engineering and biological systems), while requiring the minimum amount of power to drive the flow through the network.

To proceed, we nondimensionalize on $L_{\max}$ and κ_{wall}, defining the new quantities:

$$\hat{w} \equiv w/L_{\max}, \quad \hat{r}_j \equiv r_j/L_{\max}, \quad \hat{L} \equiv L/L_{\max},$$
$$\hat{A} \equiv A/L_{\max}^2, \quad \text{and} \quad \hat{\kappa}_j \equiv \kappa_j/\kappa_{\text{wall}}.$$

The specification of the problem can be conveniently reduced to three nondimensional parameters, the first two of which capture the asymmetry of the two fluids:

$$\beta \equiv (C_1/C_2)^2(\eta_2/\eta_1) \quad \text{and} \quad \gamma \equiv \kappa_1/\kappa_2. \tag{1}$$

We then note that if all the available volume were filled with pipes of the smallest possible radius, and the two fluids were set to uniform temperatures differing by ΔT, then there would be a maximum possible exchanged power of order $E_{\max} = \Delta T \kappa_{\text{wall}} L_{\max}^3/w^2$. Thus our last parameter is the ratio of the required exchange rate to this maximum:

$$\epsilon \equiv E_{\text{end}}/E_{\max} = Q_1 C_1 w^2/\left(L_{\max}^3 \kappa_{\text{wall}}\right), \tag{2}$$

and we typically expect $\epsilon \ll 1$.

III. OPTIMAL REGULAR EXCHANGERS

We consider a regular array of counter-flowing streams in N_j straight pipes of radii r_j ($j = 1,2$ being the two types of pipe) and length L (the same for both types), where we initially ignore any feed network to supply the individual pipes. This regular array is shown in Fig. 1(b), and we describe this array of pipes as the "active layer." since it is where exchange actually occurs.

To proceed, we make three geometric approximations: First, assuming roughly circular pipes, we approximate the total cross section (perpendicular to flow) of the array as

$$A \approx \pi N_1 (r_1 + w/2)^2 + \pi N_2 (r_2 + w/2)^2. \tag{3}$$

Second, let α be the area across which exchange occurs, then if no clustering of one type occurs α will be approximately the minimum of the two pipe perimeters, multiplied by L. We thus propose a simple approximation to the total area across which exchange occurs:

$$\alpha \approx [(N_1 2\pi r_1 L)^{-1} + (N_2 2\pi r_2 L)^{-1}]^{-1}. \tag{4}$$

Third, we approximate the thermal conductance per unit area across which exchange occurs to be

$$s \approx [(w/\kappa_{\text{wall}}) + (r_1/\kappa_1) + (r_2/\kappa_2)]^{-1}. \tag{5}$$

When is exchange complete? We assume the pipes are slender, so that heat diffusion along the length of a pipe is negligible compared to across its width (and also to advective transport along its length), and that the temperature over a cross section perpendicular to its length is roughly uniform. Let z be the distance along a pipe, with $z = 0$ being the upstream end of fluid 1 and the downstream end of fluid 2, so the average temperatures over cross sections of each of the two types of pipe are $T_j(z)$. We define the difference of inlet temperatures to be $\Delta T \equiv T_1(0) - T_2(L)$. By considering the total heat flux per unit length $J(z)$ between the two sets of pipes, we can write down the material derivative of temperature as each fluid moves along its respective pipe:

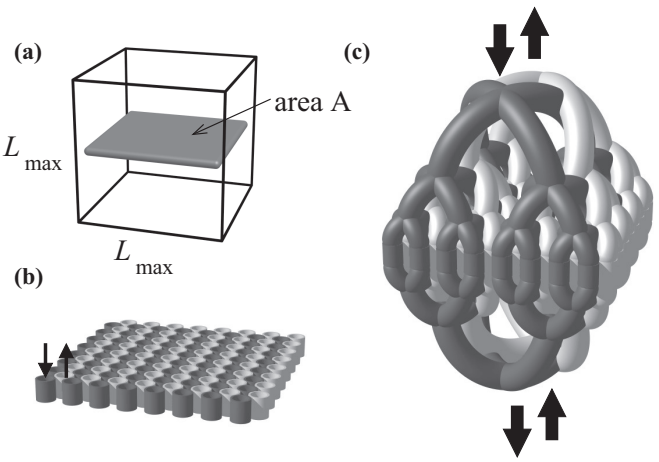

FIG. 1. (a) Schematic of the geometry of a counter-current heat exchanger "active layer" fitting inside a prescribed cubic volume of side length $L_{\max}$. (b) Detail of the active layer, showing a regular array of pipes carrying alternately counter-flowing streams. (c) The active layer connected to a branching and (on the other side) anastomosing fractal supply network.

$$\pi N_j r_j^2 C_j \frac{DT_j}{Dt} = (-)^j J(z), \tag{6}$$

where, since the average flow speed in the pipes of type $j \in \{1,2\}$ is $Q_j/(N_j \pi r_j^2)$, the material derivative is

$$\frac{D}{Dt} \equiv \frac{\partial}{\partial t} + (-)^{j+1} \frac{Q_j}{N_j \pi r_j^2} \frac{\partial}{\partial z}. \tag{7}$$

If s is the thermal conductance per unit area between pipes, we note:

$$J(z) \approx \alpha s [T_1(z) - T_2(z)]/L. \tag{8}$$

In the steady-state regime, $\partial/\partial t \equiv 0$ so Eq. (6) leads to an exchanged power E given by

$$\frac{E}{s\alpha \Delta T} = \frac{\xi_1 \xi_2 (e^{1/\xi_1} - e^{1/\xi_2})}{\xi_2 e^{1/\xi_1} - \xi_1 e^{1/\xi_2}} \approx \min(1, \xi_1, \xi_2), \tag{9}$$

$$\xi_j \equiv Q_j C_j/(\alpha s). \tag{10}$$

Complete exchange means $E \approx C_1 Q_1 \Delta T$, which from Eq. (9) is equivalent to $\xi_1 \leqslant \xi_2$ and $\xi_1 \leqslant 1$. We note from the analysis accompanying Eq. (9) that there is a special case of a balanced exchanger, in which $Q_1 C_1 = Q_2 C_2$ (so $\xi_1 = \xi_2$) and the change of temperature with z for both streams is linear, rather than being exponential. The optimal exchanger should have

this property, since otherwise some of the pipe length will contribute to dissipated power but not exchange. Thus Q_2 is determined by the imposed value of Q_1.

Now we seek to minimize the total power P required to run the exchanger, $P = Q_1\Delta p_1 + Q_2\Delta p_2$, where Δp_j are the pressures dropped across the two types of pipes. For laminar (Poiseuille [15]) flow, and using the balanced condition $Q_1C_1 = Q_2C_2$ to eliminate Q_2, we obtain

$$P = P_0\epsilon^2\hat{L}\left(\frac{1}{N_1\hat{r}_1^4} + \frac{\beta}{N_2\hat{r}_2^4}\right), \tag{11}$$

$$P_0 \equiv 8\eta_1\kappa_{\text{wall}}^2 L_{\max}^3 \big/ \left(\pi w^4 C_1^2\right). \tag{12}$$

Our task is to minimize the power P to drive the flow in Eq. (11) by choosing the five quantities N_j, $\hat{r}_j$, and $\hat{L}$, while ensuring the exchanger is compact (fits in the required volume):

$$\max(\hat{r}_j) \leqslant \hat{L} \leqslant 1, \tag{13}$$

$$\hat{A} = \pi N_1(\hat{r}_1 + \hat{w}/2)^2 + \pi N_2(\hat{r}_2 + \hat{w}/2)^2 \leqslant 1, \tag{14}$$

and also that exchange is complete, which from $\xi_1 \leqslant 1$ and Eqs. (4), (5), and (10) leads to

$$\frac{\epsilon}{\hat{w}^2 2\pi\hat{L}}\left(\frac{1}{N_1\hat{r}_1} + \frac{1}{N_2\hat{r}_2}\right)\left(\hat{w} + \frac{\hat{r}_1}{\hat{\kappa}_1} + \frac{\hat{r}_2}{\hat{\kappa}_2}\right) \leqslant 1. \tag{15}$$

The optimization can then be performed numerically with the constraints (13), (14), and (15). We do this in two different ways, which give essentially identical results: we either repeatedly choose a random direction in the five-dimensional space of $(N_j,\hat{r}_j,\hat{L})$ and follow this direction until either the dissipated power does not fall or a constraint is encountered; or, we impose completeness of exchange in Eq. (15) as an equality, which allows us to determine $\hat{L}$ given the other variables, and then perform an exhaustive search for the minimum power over the more tractable four-dimensional space $(N_j,\hat{r}_j)$.

Table I shows the geometry of some optimized regular exchangers for real cases, and the optimized results are included in Fig. 2 with the label "regular."

TABLE I. Estimated parameters for various real systems. "S.I." refers to the international system of units; so for thermal systems C will have units J m^{-3} K^{-1} and κ will have units W m^{-1} K^{-1}. For gas exchange, C will have units kilogram of relevant gas per m^3 of fluid, per Pascal of partial pressure, and κ will have units kg s^{-1} m^{-1} Pa^{-1} (so that κ/C is a diffusivity). "T.E.G." is thermoelectric generation from internal combustion engine exhaust [14] (we have chosen values corresponding to a car or personal automobile). For the animal respiratory systems we assume that transport across the exchange membrane is similar to that of water. For blood, we assume that oxygen can exist in a mobile form (dissolved in the waterlike serum) and an immobile form (bound to hemoglobin). Thus the oxygen "conductivity" κ_1 for blood is the same as for water, while C_1 is increased over that of water by the carrying capacity of heme. Data are from Refs. [16–20]. Results for a regular exchange network are indicated by the subscript "reg"; while the results for the fractal exchange surfaces (denoted by a subcript "frac") use a Hausdorff dimension $d = 2.33$. For the cases of pigeon and salmon respiration, we impose the additional constraint that $r_1 > 5\ \mu$m, in order to allow erythrocytes to pass through blood vessels (type 1 pipes). This appears to only affect the fractal case, and without this requirement, the optimized value of r_1 for this fractal case would be 1.5 and 0.4 μm for pigeon and salmon, respectively. We have also ignored the non-Newtonian nature of blood rheology (small for blood plasma [21]) and the possibility for soft particles (and even simple nonlinearities [22]) to cause complex [23] and even chaotic flows [24].

System:	T.E.G.	Pigeon	Salmon
Exchanged:	Heat	Oxygen	Oxygen
$L_{\max}$/m	2.0×10^{-1}	5.0×10^{-2}	2.0×10^{-2}
w/m	5.0×10^{-4}	5.0×10^{-7}	5.0×10^{-7}
Q_1/m^3 s^{-1}	5.0×10^{-2}	2.0×10^{-5}	1.0×10^{-6}
C_1/S.I.	1.0×10^{3}	2.0×10^{-6}	2.0×10^{-6}
C_2/S.I.	1.0×10^{3}	1.3×10^{-5}	1.0×10^{-7}
κ_1/S.I.	4.0×10^{-2}	1.8×10^{-16}	1.6×10^{-16}
κ_2/S.I.	4.0×10^{-2}	2.3×10^{-10}	1.6×10^{-16}
κ_{wall}/S.I.	1.0×10^{1}	1.8×10^{-16}	1.6×10^{-16}
η_1/Pa s	4.0×10^{-5}	4.0×10^{-3}	4.0×10^{-3}
η_2/Pa s	4.0×10^{-5}	4.0×10^{-5}	1.0×10^{-3}
β	1.0×10^{0}	2.4×10^{-4}	1.0×10^{2}
γ	1.0×10^{0}	7.8×10^{-7}	1.0×10^{0}
ϵ	1.6×10^{-4}	4.4×10^{-4}	3.9×10^{-4}
$r_{1,\text{reg}}$/m	1.0×10^{-3}	2.5×10^{-5}	5.2×10^{-6}
$r_{2,\text{reg}}$/m	1.0×10^{-3}	2.2×10^{-6}	2.1×10^{-5}
A_{reg}/m^2	4.0×10^{-2}	2.5×10^{-3}	4.0×10^{-4}
L_{reg}/m	2.0×10^{-1}	5.0×10^{-2}	2.0×10^{-2}
P_{reg}/W	2.4×10^{1}	6.2×10^{-1}	7.7×10^{-1}
$r_{1,\text{frac}}$/m	5.1×10^{-4}	5.0×10^{-6}	5.0×10^{-6}
$r_{2,\text{frac}}$/m	5.1×10^{-4}	5.4×10^{-7}	7.3×10^{-6}
A_{frac}/m^2	6.6×10^{-2}	1.0×10^{-2}	7.6×10^{-4}
L_{frac}/m	4.3×10^{-2}	7.1×10^{-4}	2.9×10^{-3}
P_{frac}/W	1.8×10^{1}	6.0×10^{-2}	4.0×10^{-1}

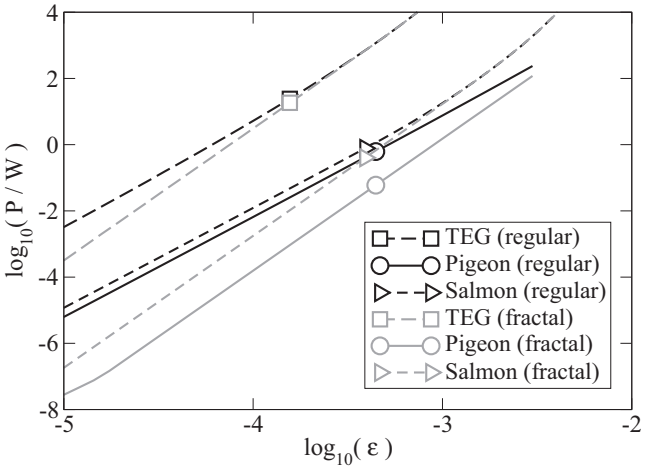

FIG. 2. Plots of power dissipated in exchange for the three cases of Table I. Here we change Q_1 to achieve different values of ϵ. The actual cases in Table I are shown as symbols. For the cases of "pigeon" and "salmon," we additionally impose the constraint that blood vessels (type 1 pipes) should be large enough to carry erythrocytes (taken as the condition $r_1 > 5\ \mu$m).

IV. SCALING OF REGULAR EXCHANGERS AND LIMITING CONDITIONS

It is interesting to look at what limits the exchanger efficiency in different cases. For the examples studied here, the numerical results show that over essentially the entire range of ϵ, Eqs. (14) and, unsurprisingly, (15) are satisfied as equalities. Furthermore, $\hat{w}$ is typically much less than $\hat{r}_j$ or $\hat{r}_j/\hat{\kappa}_j$.

For symmetric exchangers, where $N_1 = N$, $\hat{r}_1 = \hat{r}_2$, and $\hat{\kappa}_1 = \hat{\kappa}_2$, we can see the consequences of this for the scaling behavior with ϵ, because Eqs. (14) and (15) reduce to

$$2\pi N_1 \hat{r}_1^2 \approx 1 \quad \text{and} \quad \frac{\epsilon}{\hat{w}^2 2\pi \hat{L}} \frac{2}{N_1 \hat{r}_1} \frac{2\hat{r}_1}{\hat{\kappa}_1} \approx 1, \tag{16}$$

which implies the dissipated power

$$P \approx 16\pi P_0 \epsilon^3/(\hat{\kappa}_1 \hat{w}^2). \tag{17}$$

Two observations follow from this rough analysis: First, the dissipated power in this approximation does not depend on $\hat{L}$, so that although the numerical results indicate that optimization pushes $\hat{L}$ towards unity, this is only a weakly selected result. Thus exchangers with very similar dissipated power can be made from rather thin active layers [as shown schematically in Fig. 1(b)] without incurring a strong penalty. This is useful in allowing room for the supply network that we will wish to attach to the active layer.

Second, an interesting question to ask for an optimal exchange network is, which constraint is significantly limiting the performance? The nontrivial constraint in this case is typically the area $\hat{A}$ of the active layer in Eq. (14), which we would prefer to make larger than $L_{\max}^2$.

Taken together, these observations imply that a route to further optimization is to have an active layer which is both thin and also folded in some way to accommodate a larger area inside the prescribed volume of the device, an approach we will pursue further in Sec. VI below.

V. THE BRANCHED SUPPLY NETWORK

So far, we have considered the active layer of the exchanger as an independent entity. However, it must be supplied with the two working fluids, and for the optimization scheme above to be relevant, this supply network, which dissipates power but performs no significant exchange, should not dominate the power consumption of the whole device.

Consider therefore a branched (and fractal) supply network shown in Fig. 1(c), which brings the streams to the exchanger's active layer. In contrast to Ref. [2], we do not need the supply network to pass close to every point in space. Suppose that each pipe comprising the supply network branches into b smaller pipes at each hierarchical level k of the tree (where pipes with higher values of k are smaller, and closer to the active layer where exchange occurs). Let the ratio of pipe radii between neighboring levels be $\rho < 1$, and the ratio of pipe lengths be λ. The ratio of power dissipated between hierarchical levels is therefore

$$P_{k+1}/P_k = \lambda/(b\rho^4). \tag{18}$$

Since the active layer is densely covered with pipes, the condition to fit the supply network into space is $\rho \geqslant b^{-1/2}$. Therefore, provided $\lambda > b\rho^4$, the power will increase exponentially with k and the overall power dissipation in the supply network will be of the order of that in the last layer, and therefore of the same order as in the active layer. The supply network will therefore not dominate the power dissipation.

As an example from biology, for the human arterial system Murray [25] proposed the law that at a branch point, the sum of the cube of diameters of outgoing vessels is equal to the cube of the incoming vessel. Thus for binary branching (i.e., $b = 2$), $\rho = 2^{-1/y}$ with $y = 3$. If vessel lengths are proportional to their diameter [26] we obtain $P_{k+1}/P_k = 2^{(3/y)-1}$. For Murray's original law, this would imply $P_{k+1}/P_k = 1$ and ignoring the supply network would be invalid. However, experimentally it is found that for arteries (see [26,27], and references therein) that y is in the range 2.6–2.7, except in capillary beds, so our analysis may still be applicable.

VI. FRACTAL EXCHANGE NETWORKS

From the solution above for optimum regular exchange networks, the lateral cross section A always expands to its maximum value $L_{\max}^2$. If this restriction were lifted, a more efficient exchanger would likely be possible. This can be achieved by allowing the active layer (provided it is thin enough, and can still be provided with a branching supply network) to be corrugated, while still fitting within the prescribed roughly cubical volume $L_{\max}^3$ available. One way to do this is to turn the active layer into an approximation to a fractal surface. Thus suppose the active layer to be corrugated into such a fractal surface over a range of lateral length scales down to a scale $x \geqslant L$ (where L is the pipe length, and therefore the thickness of the layer). In the limit $x \to 0$ the surface would have some Hausdorff dimension [28], which we denote d. Figure 3 shows schematically an example in which the surface is the type I quadratic Koch surface with (in the limit) Hausdorff dimension $d_{\text{Koch}} = \ln 13/\ln 3 \approx 2.33$. Let the area of the active layer be $A(x)$, where

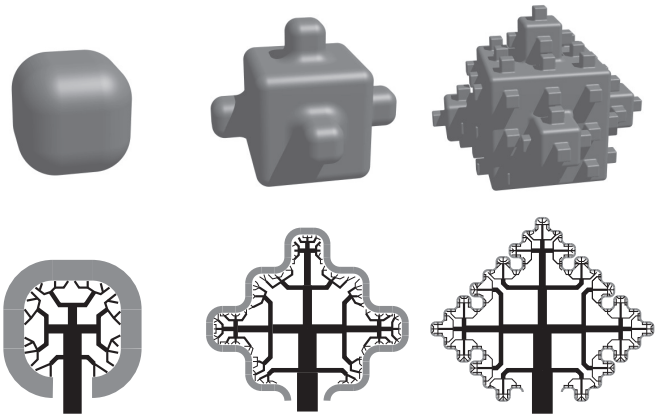

FIG. 3. Top row: Schematic of the active layer of Fig. 1(a), corrugated into a hierarchical (fractal) surface, comprising (left to right) greater area and more iterations of the fractal. Bottom row: Schematic section through these surfaces showing the fractal supply network in the interior (the corresponding network outside is not shown, and will require a more complex design to ensure equal flow to all parts of the active layer).

$A(L_{\max}) = L_{\max}^2$, then from Hausdorff's definition of dimension, we see that $A(x) = L_{\max}^2 (x/L_{\max})^{2-d}$. We can therefore replace the inequality $\hat{A} \leqslant 1$ in Eq. (14) by

$$\hat{A} = \pi N_1 (\hat{r}_1 + \hat{w}/2)^2 + \pi N_2 (\hat{r}_2 + \hat{w}/2)^2 \leqslant \hat{L}^{2-d}. \quad (19)$$

Figure 2 shows the effect of ϵ (varied through altering Q_1) on the power dissipation for fractal exchangers corresponding to the scenarios in Table I, compared to that of the regular exchanger. Corrugating the exchange layer into a type I quadratic Koch surface leads to a significant reduction in the dissipated power for the two biological cases (factor gain of 10 for pigeon lungs and 2 for salmon gills). However, the small size of the optimum pipe radii r_1 may mean that this degree of optimization is precluded by other considerations. For instance, erythrocytes need to be able to pass through these type 1 (blood carrying) vessels.

Crumpling the active layer into a (limited length scale) fractal surface would also be expected to produce a novel scaling of dissipated power with ϵ. The numerical results indicate that in the optimum exchanger $\hat{A}$ expands to its new maximum extent, so Eq. (19) is an equality. As above, Eq. (15) is an equality, but we find for the TEG case that $\hat{w}$ is comparable to $\hat{r}_j$, while $\hat{w}$ remains substantially less than $\hat{r}_j/\hat{\kappa}_j$. This leads in the symmetric case to the following versions of Eqs. (19) and (15):

$$\frac{9\pi}{4} N_1 \hat{w}^2 \approx \hat{L}^{2-d} \quad \text{and} \quad \left(\frac{2\hat{r}_1}{\hat{\kappa}_1}\right)\left(\frac{2}{N_1 \hat{r}_1}\right) \approx \frac{2\pi \hat{L} \hat{w}^2}{\epsilon} \quad (20)$$

(the first assuming for definiteness $\hat{w} \approx \hat{r}_1$), which implies the dissipated power is

$$P \approx \left(\frac{9}{2}\right)^{2/(3-d)} \frac{\pi P_0}{\hat{w}^2} \hat{\kappa}_1^{(1-d)/(3-d)} \epsilon^{(5-d)/(3-d)}. \quad (21)$$

For the quadratic Koch surface, this leads to $P \propto \epsilon^{4.01}$, which is close to the observed exponent in Fig. 2. We also note that $\hat{L} \propto \epsilon^{1/(3-d)}$, which increases with ϵ.

As the fractal dimension d of the active layer is increased towards the upper limit of 3, the dissipated power P is likely to fall. However, the assumptions that were used to derive Eq. (21), namely, $\hat{w} \approx \hat{r}_j \ll \hat{r}_j/\hat{\kappa}_j$, may at some point cease to be valid, so the scaling of P with d in Eq. (21) will break down at a point which is case specific. For example, in the human pulmonary system (although not a counter-current network and not symmetric), the fractal dimension of the set of alveoli is believed to be three down to small scales [29] (Hou *et al.* [30] provide arguments that this is optimal). Equation (21) becomes singular in the limit $d \to 3$, so cannot apply, although we believe Eqs. (11), (12), (13), (15), and (19) should still hold if a suitable supply network can be designed.

VII. CONCLUSIONS

Exchange networks of the class we show here exhibit broadly power-law dependence of the dissipated power with the quantity ϵ, which measures the required throughput: the rate of exchange of heat, gas, or solute needed. This is true both for a fractally corrugated or a simple regular array of exchange pipes. However, the fractal exchangers demonstrate gains in efficiency when compared to regular exchangers for small values of ϵ, and in particular for parameters relevant to biological systems. This is driven by the higher efficiency of a thin active exchange layer of large area; the fractal corrugations being one way to accommodate this geometry in a compact volume. At higher throughput (larger ϵ) the optimal thickness of the active layer increases, so the number of fractal generations in the corrugations falls. Because of this, the dissipated power converges towards the value for the regular exchange network.

We note that the analysis we have performed here aims specifically to minimize required power while ensuring complete exchange has taken place and compactness of the exchange device. In practice, other design constraints may need to be included; for example, a requirement that the network be robust [3] or easily repairable [31,32] under external attack [33,34]; or the cost of building the network may be significant compared to its operating costs [35,36]. Nevertheless, the conditions analyzed here are, we believe, relevant to a wide class of engineering and biological systems and could provide the basis for improved industrial efficiency and insights into the structures used for respiration in the living world.

[1] D. W. Green and R. H. Perry, *Perry's Chemical Engineers' Handbook*, 8th ed. (McGraw-Hill, New York, 2007).

[2] G. West, J. H. Brown, and B. J. Enquist, A general model for the origin of allometric scaling laws in biology, Science **276**, 122 (1997).

[3] E. Katifori, G. J. Szöllösi, and M. O. Magnasco, Damage and fluctuations induce loops in optimal transport networks, Phys. Rev. Lett. **104**, 048704 (2010).

[4] A. N. Makanya and V. Djonov, Development and spatial organization of the air conduits in the lung of the domestic fowl, *Gallus gallus* variant *domesticus*, Microsc. Res. Tech. **71**, 689 (2008).

[5] B. M. Wiebe and H. Laursen, Human lung volume, alveolar surface area, and capillary length, Microsc. Res. Tech. **32**, 255 (1995).

[6] D. Hunt and V. M. Savage, Asymmetries arising from the space-filling nature of vascular networks, Phys Rev. E **93**, 062305 (2016).

[7] P. S. Dodds, Optimal form of branching supply and collection networks, Phys. Rev. Lett. **104**, 048702 (2010).

[8] R. Hague and P. Reeves, Additive manufacturing and 3D printing, Ingenia 55, June (2013).

[9] D. B. Tuckerman and R. F. W. Pease, High-performance heat sinking for VLSI, Electron Device Lett. **2**, 126 (1981).

[10] A. Bejan and M. R. Errera, Deterministic tree networks for fluid flow: Geometry for minimal flow resistance between a volume and one point, Fractals **05**, 685 (1997).

[11] Y. Chen and P. Cheng, Heat transfer and pressure drop in fractal tree-like microchannel nets, Int. J. Heat Mass Transf. **45**, 2643 (2002).

[12] W. Escher, B. Michel, and D. Poulikakos, Efficiency of optimized bifurcating tree-like and parallel microchannel networks in the cooling of electronics, Int. J. Heat Mass Transf. **52**, 1421 (2009).
[13] A. Bejan and Y. Fautrelle, Constructal multi-scale structure for maximal heat transfer density, Acta Mech. **163**, 39 (2003).
[14] M. V. Twigg, Progress and future challenges in controlling automotive exhaust gas emissions , Appl. Catal., B **70**, 2 (2007).
[15] E. Hagenbach, Ueber die Bestimmung der Zähigkeit einer Flüssigkeit durch den Ausfluss aus Röhren, Ann. Phys. (Berlin) **185**, 385 (1860).
[16] *Handbook of Chemistry and Physics*, 75th ed., edited by D. R. Lide (CRC Press, Boca Raton, FL, 1995).
[17] E. L. Cussler, *Diffusion: Mass Transfer in Fluid Systems*, 2nd ed. (Cambridge University Press, New York, 1997).
[18] K. Schmidt-Nielsen, *Animal Physiology: Adaptation and Environment* (Cambridge University Press, Cambridge, 1990).
[19] P. J. Butler, N. H. West, and D. R. Jones, Respiratory and cardiovascular responses of the pigeon to sustained, level flight in a wind-tunnel, J. Exp. Biol. **71**, 7 (1977).
[20] J. W. Kicenuik and D. R. Jones, The Oxygen transport system in trout (*Salmo gairdneri*) during sustained exercise, J. Exp. Biol. **69**, 247 (1977).
[21] M. Brust, C. Schaefer, R. Doerr, L. Pan, M. Garcia, P. E. Arratia, and C. Wagner, Rheology of human blood plasma: Viscoelastic versus Newtonian behavior, Phys. Rev. Lett. **110**, 078305 (2013).
[22] J. B. Geddes, B. D. Storey, D. Gardner, and R. T. Carr, Bistability in a simple fluid network due to viscosity contrast, Phys. Rev. E **81**, 046316 (2010).
[23] F. Jousse, R. Farr, D. R. Link, M. J. Fuerstman, and P. Garstecki, Bifurcation of droplet flows within capillaries, Phys. Rev. E **74**, 036311 (2006).
[24] A. B. Schelin, G. Karolyi, A. P. S. de Moura, N. A. Booth, and C. Grebogi, Chaotic advection in blood flow, Phys. Rev. E **80**, 016213 (2009).
[25] C. D. Murray, The physiological principle of minimum work: I. The vascular system and the cost of blood volume, Proc. Natl. Acad. Sci. **12**, 207 (1926).
[26] E. Gabryś, M. Rybaczuk, and A. Kędzia, Fractal models of circulatory system. Symmetrical and asymmetrical approach comparison, Chaos, Solitons Fractals **24**, 707 (2005).
[27] M. Changizi and C. Cherniak, Modeling the large-scale geometry of human coronary arteries, Can. J. Physiol. Pharmacol. **78**, 603 (2000).
[28] F. Hausdorff, Dimension und äußeres Maß, Math. Ann. **79**, 157 (1918).
[29] B. B. Mandelbrot, *The Fractal Geometry of Nature* (Freeman, San Francisco, 1982), p. 157.
[30] C. Hou, S. Gheorghui, M. O. Coppens, V. H. Huxley, and P. Pfeifer, in *Fractals in Biology and Medicine*, edited by G. A. Loser, D. Merlini, T. F. Nonnenmacher, and E. R. Weibel (Springer, New York, 2005), pp. 17–30.
[31] W. Quattrociocchi, G. Caldarelli and A. Scala, Self-healing networks: Redundancy and structure, PLoS One **9**, e87986 (2014).
[32] R. S. Farr, J. L. Harer, and T. M. A. Fink, Easily repairable networks: Reconnecting nodes after damage, Phys. Rev. Lett. **113**, 138701 (2014).
[33] R. Cohen, K. Erez, D. ben-Avraham, and S. Havlin, Resilience of the Internet to random breakdowns, Phys. Rev. Lett. **85**, 4626 (2000).
[34] R. Cohen, K. Erez, D. ben-Avraham, and S. Havlin, Breakdown of the internet under intentional attack, Phys. Rev. Lett. **86**, 3682 (2001).
[35] S. Bohn and M. O. Magnasco, Structure, scaling, and phase transition in the optimal transport network, Phys. Rev. Lett. **98**, 088702 (2007).
[36] M. Durand, Structure of optimal transport networks subject to a global constraint, Phys. Rev. Lett. **98**, 088701 (2007).